IEEE Access
Multidisciplinary | Rapid Review | Open Access Journal

Received June 17, 2021, accepted July 18, 2021, date of publication August 2, 2021, date of current version August 11, 2021.

Digital Object Identifier 10.1109/ACCESS.2021.3101890

A Diagnosis Method of Semiconductor Power Switch Open-Circuit Fault in the PMSM Drive System With the MPCC Method

HAI YU, JUNJUN DENG, (Member, IEEE), AND YANG LI
Collaborative Innovation Center of Electric Vehicles in Beijing, Beijing 100081, China
Beijing Institute of Technology, Beijing 100081, China

Corresponding author: Junjun Deng (dengjunjun@bit.edu.cn)

This work was supported by the National Key Research and Development Program of China under Grant 2019YFB1600800.

ABSTRACT The model predictive current control (MPCC) method has been widely used in permanent magnet synchronous motor (PMSM) drive systems for excellent dynamic performance. The fault diagnosis of the PMSM drive system becomes as important as dynamic performance improvement. The open-circuit fault of the semiconductor power switches is commonly seen in the PMSM drive system, which causes safety issues due to the abnormal operation of the system if the fault has not been detected. However, the previous fault diagnosis methods are mainly aimed at PMSM drive systems with conventional control methods. Focused on PMSM drive system with MPCC method, a diagnosis method of semiconductor power switch open-circuit fault has been proposed. The calculated result of the cost function in implementing the MPCC algorithm has been picked as the primary characteristic parameter for fault diagnosis, which is derived through comparative analysis of the operation in fault conditions with normal conditions. In addition, the monitored stator current and the gate-driving signals of the switches are used as subordinate fault characteristic parameters. The selected three fault indices together with a digital filtering algorithm complete the switches' open-circuit fault diagnosis. A MATLAB/Simulink model has been built to validate the effectiveness of the proposed fault diagnosis method. The simulation results verify the proposed method's robustness against the operating point and parameter mismatch of the PMSM drive system.

INDEX TERMS Fault diagnosis, MPCC method, PMSM drive system, semiconductor power switch.

I. INTRODUCTION

The permanent magnet synchronous motor (PMSM) has been widely used in electric vehicles, aircraft, and other industrial fields due to its high power density, high torque density, and high efficiency [1]–[3]. The PMSM drive systems working in complicated conditions hold a high risk of failures during the long-term operation process [4]. An undetected fault of the drive system, which leads to an abnormal operation, brings economic losses and even safety issues. Therefore, the fault diagnosis for the PMSM drive system is necessary and helpful to schedule preventive maintenance to avoid such catastrophes [5], [6].

The inverter, which is mainly composed of semiconductor power switches, is the vulnerable part of the PMSM drive system [7]. Semiconductor power switch faults mainly include short-circuit faults and open-circuit faults. When a short-circuit fault occurs, a large inrush current is generated in the system, which causes serious consequences. Therefore, the overcurrent protection circuits are usually designed in the inverter. On the other hand, the switches' open-circuit fault does not lead the PMSM drive system to stop running immediately. However, it deteriorates the system's performance. Therefore, an effective diagnosis method for the open-circuit fault is of great significance to the safety of the motor drive system. At present, there are mainly three types of diagnosis methods for switches' open-circuit fault [8], [9]: model-based, signal-based, and knowledge learning.

For the model-based fault diagnosis method, firstly, a specific model is established according to the working principle of the PMSM drive system. Then, the estimated value of the fault characteristic parameter is obtained through the observer

The associate editor coordinating the review of this manuscript and approving it for publication was Dazhong Ma.

or other methods, which is compared with the reference value to calculate the residual. Third, the calculated residual is compared with a threshold to detect whether the fault occurs. This type of fault diagnosis method holds a good dynamic response, which is considered suitable for operating conditions where torque and speed vary. Specifically, the observer-based method is applied to diagnose the open-circuit fault in [10]–[14]. In [12], a novel open switch fault diagnosis method based on the differential current observer is proposed. To avoid false and missed detection caused by the change of operating conditions, an adaptive fault detection threshold is designed. In [13], to quickly diagnose whether the fault occurs, a current estimator was constructed based on the healthy hybrid system model. The fault isolation can be carried out according to the characteristics of Euclidean distances. In [14], an effective open-switch fault detection method based on the Kalman filter algorithm is proposed for PMSM drives with open-loop or closed loop control strategies. In [15], a small-signal modeling approach based on the characteristic equation for converter-dominated islanded ac microgrid is used to assess the system's low-frequency stability. However, these methods require high-quality sensor signals and accurate system model parameters.

The signal-based fault diagnosis method does not rely on the PMSM drive system's model and its parameters. It extracts the sensors' signal characteristics of the fault system. Then the correlation between the signal characteristics and the fault is analyzed for fault diagnosis. In the PMSM drive system, the voltage signals and the current signals are usually used for switches' fault diagnosis. The voltage is categorized as the controlled variable, while the current is the response variable. Compared with the fault diagnosis method based on current signal analysis, the diagnosis speed of the voltage signal-based method is faster. However, the voltage signal-based fault diagnosis method requires additional hardware circuits such as voltage sensors, which increases complexity and cost. The key of the current signal-based fault diagnosis method is the current signal extraction for the fault characteristic. The average value of the current park vector is picked as the fault characteristic parameter in [16], which is not suitable when the load varies. To deal with load variation, the normalized DC method is proposed, which takes the ratio of the average value of phase current over one period to the average value of its fundamental harmonic as the fault index in [17]. Subsequently, the normalized DC method is modified in [18] to be applied in the closed-loop control system. Furthermore, In speed-controlled motor drive systems, the average absolute value of the normalized current has been combined with its average value to diagnose multiple power switches' open-circuit faults in [19], [20], which shows immunity to false alarms. In the torque-controlled motor drive system, the difference between the actual values and the referential values of current through the three phases were calculated by the sampled data acquired in a variable sliding observation window, which is utilized in single switch's open-circuit fault diagnosis in [21]. In addition to the diagnostic variable based on the three-phase stator current over an electrical cycle, the auxiliary diagnostic variable, which is based on the cross-comparison of the three-phase stator current, is presented and used to diagnose multiple open circuit faults in insulated gate bipolar transistors [22]. In short, more attention has been drawn to the diagnosis of multiple power switchers' open-circuit faults. In [23], a new reliable approach, based on the average normalized value of the product of the two stator currents and the polarity of the normalized average current, is proposed to diagnosis current sensor faults and power semiconductor open-circuit faults in PMSM drives.

The fault diagnosis method based on knowledge learning transforms the mapping relationship between the fault data and the fault characteristics into the stored fault diagnosis knowledge, which is expressible for completing the fault diagnosis process. This type of fault diagnosis method does not focus on the analysis of the working principle and failure mechanism of the PMSM drive system, which gives full play to the advantages of the knowledge learning method. The fuzzy logic method has been applied in analyzing the current signals for the diagnosis of power switch open-circuit fault in [24], [25]. However, the designer's experience affects the selection of fuzzy sets and membership functions in fuzzy logic methods, which has an impact on the accuracy of the fault classification. In [26], a generative adversarial network based on tri-networks form (tnGAN) with incomplete sensor data is used to handle leak detection problems for the pipeline network. The amount of data collected is large, and there may be a redundancy of data information, affecting detection time. In [27], the double chain quantum genetic algorithm is employed to obtain the proper length of measured signals and the deep belief networks (DBN) structure parameters. Then, the fault features are extracted from the signals through DBN, and used to train the least square support vector machine (LSSVM) fault classifier to complete fault diagnosis. In [28], compared with recurrent neural network and LSSVM, the long short-term memory network, which excavates the deep information of the fault signal with the highest diagnosis accuracy and strongest robustness with short time delay, is used to detect multiple open-circuit switch faults. In addition, there are also fault diagnosis methods based on knowledge learning combined with signal time-frequency feature analysis. In [29], the wavelet transform is used to extract the feature of fault, which is respectively combined with the neural network and support vector machine to complete the fault diagnosis. However, the overall operating conditions should be divided into specific segments using the wavelet transform. Besides, the neural network and support vector machine require a lot of training sample data, which keeps it away from popularization. In [30], the fast Fourier transform is used to extract the signal features, the principal component analysis method is used to reduce the dimension of the samples, and the Bayesian network is used for fault detection and diagnosis. However, the fast Fourier transform is preferable for the frequency characteristic extraction of

the stationary signal analysis, and the computational complexity of this method is relatively high, which calls for high-performance processors. Recently, based on the explicit analytical model of converters and the learning capability of the artificial neural network, a model-data-hybrid-driven (MDHD) method is proposed to diagnose open-switch faults in power converters [31].

Meanwhile, the fault diagnosis method may be different considering the characteristics of the different control methods applied in the PMSM drive system. The diagnosis of power switch open-circuit fault presented in the previous literature review is suitable for the PMSM drive system with the conventional control method. In recent years, the finite control set model predictive control (FCS-MPC) method is widely used in the PMSM drive system due to its simple structure and excellent dynamic performance [32]–[34]. According to the control variables in the PMSM drive system, the FCS-MPC is divided into model predictive current control (MPCC) and model predictive torque control (MPTC) [35], [36]. The MPCC method is relatively widely applied in the PMSM drive system. The fault diagnosis research of the PMSM drive system with the FCS-MPC method is getting more and more attention [37]–[40]. In [37], the DC component and second harmonic component in the cost function are used for the open-phase fault diagnosis, and the initial phase angle differences are defined to identify the faulty phase. In [38], the wavelet transform is applied to extract the fault feature from the cost function existing in the MPC system, and the inter-turn fault is diagnosed by monitoring the normalized energy-related feature vector calculated from the wavelet transform coefficients. In [39], the errors between the reference currents and the PMSM stator predictive currents are used to generate appropriate diagnostic variables, which is combined with the fuzzy logic approach to identify the faulty power switches. In [40], the detection is implemented through the normalized average value of cost function variation over a fundamental period. Besides, the open-circuit fault diagnosis is realized using the $\alpha\beta$-current signatures. In the open-circuit fault diagnosis of the three phase voltage source inverters, there are few studies to analyze the changes of the fault signals according to control strategies.

Therefore, this paper based on the fault signal analysis proposes a diagnosis method of semiconductor power switch open-circuit fault for the PMSM drive system with the MPCC method. The abnormality of the PMSM drive system is detected by the cost function, and the faulty switch is identified based on the stator current and the drive signal of the power switcher. This method does not require additional hardware and makes full use of the signals in the control strategy, including cost function, three-phase current, and driving signals. In addition, it is robust against the operating point and parameter mismatch of the PMSM drive system. The remainder of this paper is organized as follows. In section II, the MPCC method of the PMSM drive system is described. In section III, the open-circuit fault signal of the semiconductor power switch is analyzed. In section IV, fault detection and identification are described. In section V, the simulation result validation is carried out. In section VI, the conclusion is drawn.

II. MPCC OF PMSM DRIVE SYSTEM

To facilitate the research of the fault diagnosis method, the MPCC is briefly described in this section.

A. PMSM MODEL UNDER HEALTHY CONDITION

In the dq-axis coordinate system, the voltages of the three-phase PMSM can be expressed as

$$\begin{cases} u_d = R_s i_d + L_d \dfrac{di_d}{dt} - \omega_e L_q i_q \\ u_q = R_s i_q + L_q \dfrac{di_q}{dt} + \omega_e L_d i_d + \omega_e \psi_m \end{cases} \tag{1}$$

where u_d and u_q are the dq-axis voltages, i_d and i_q are the dq-axis stator currents, L_d and L_d are the dq-axis inductances, R_s is the stator resistance, ψ_m is the permanent magnet flux linkage, ω_e is the electrical angular velocity.

The electromagnetic torque of the three-phase PMSM is expressed as

$$T_e = \frac{3}{2} p(\psi_m i_q + (L_d - L_q) i_d i_q) \tag{2}$$

where T_e is the electromagnetic torque, p is the number of pole pairs.

B. MPCC METHOD

1) PREDICTIVE MODEL

In the dq-axis coordinate system, i_d is proportional to the reactive power and i_q proportional to the electromagnetic torque. Euler approximation method is used for stator current derivative as follows

$$\frac{di}{dt} \approx \frac{i(k+1) - i(k)}{T_s} \tag{3}$$

where T_s is the sample time.

Therefore, the prediction model of the stator currents can be expressed as

$$\begin{cases} i_d^p(k+1) = (1 - \dfrac{R_s T_s}{L_d}) i_d(k) \\ \quad + \dfrac{\omega_e(k) L_q T_s i_q(k)}{L_d} + \dfrac{T_s u_d(k)}{L_d} \\ i_q^p(k+1) = (1 - \dfrac{R_s T_s}{L_q}) i_q(k) \\ \quad - \dfrac{\omega_e(k) L_d T_s i_d(k)}{L_q} \\ \quad + \dfrac{T_s u_q(k)}{L_q} - \dfrac{\omega_e(k) \psi_m T_s}{L_q} \end{cases} \tag{4}$$

where $i_d(k)$ and $i_q(k)$ are the measured values of the dq-axis stator currents, $u_d(k)$ and $u_q(k)$ are the calculated values of the dq-axis voltages, $\omega_e(k)$ is the electrical angular velocity, all the above values are sampled in the k^{th} interval. $i_d^p(k+1)$ and $i_q^p(k+1)$ are the predicted values of the dq-axis stator currents in the $(k+1)^{th}$ sample interval.

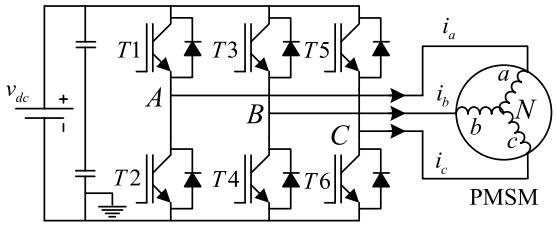

FIGURE 1. Structure of the two-level voltage source inverter.

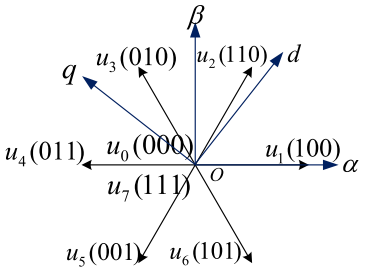

FIGURE 2. Voltage vectors.

2) COST FUNCTION

The two-level voltage source inverter is adopted in the investigated PMSM drive system as shown in Fig. 1, where the corresponding semiconductor power switches are named T1-T6. Thus, there are eight voltage vectors used for the MPCC method, as shown in Fig. 2.

In the MPCC method, the cost function is defined to force the stator current to track the reference value. The voltage vector minimizing the cost function is applied to the motor drive system in the next sampling period. The cost function is defined as

$$g_i = [i_d^*(k+1) - i_d^p(k+1)]^2 + [i_q^*(k+1) - i_q^p(k+1)]^2 + g[i_d^p(k+1), i_q^p(k+1)] \quad (5)$$

where $i = 0, 1, 2, \ldots, 7$, $i_d^*(k+1)$ and $i_q^*(k+1)$ denote the reference values of the dq-axis stator currents in the $(k+1)^{th}$ sample interval. In (5), the first term represents to minimize the reactive power. The second term represents to track the reference torque. The last term is a nonlinear function to limit the amplitude of the stator currents. The nonlinear function is expressed as

$$g[i_d^p(k+1), i_q^p(k+1)] = \begin{cases} \infty & (|i_d^p(k+1)| > i_{\max} \text{ or } |i_q^p(k+1)| > i_{\max}) \\ 0 & (|i_d^p(k+1)| \le i_{\max} \text{ and } |i_q^p(k+1)| \le i_{\max}) \end{cases} \quad (6)$$

where $i_{\max}$ is the maximum value of the amplitudes of the stator currents.

In the practical PMSM drive system, there is usually one beat delay due to the algorithm operation and power switch action, which can deteriorate the performance of the MPCC method, such as the increased current ripple. So, it is necessary to compensate for the time delay [41]. Supposing that the delay is one switching period in this paper, the cost function is redefined as

$$g_i = [i_d^*(k+2) - i_d^p(k+2)]^2 + [i_q^*(k+2) - i_q^p(k+2)]^2 + g[i_d^p(k+2), i_q^p(k+2)] \quad (7)$$

where $i_d^*(k+2)$ and $i_q^*(k+2)$ are the reference values in the $(k+2)^{th}$ sample interval, $i_d^p(k+2)$ and $i_q^p(k+2)$ are the predicted values in the $(k+2)^{th}$ sample interval. In addition, Fig. 3 shows the MPCC block diagram of the PMSM drive system.

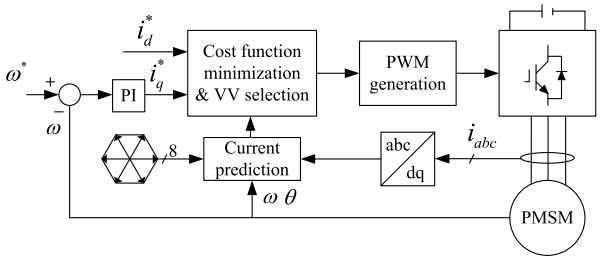

FIGURE 3. MPCC block diagram of the PMSM drive system.

C. PARAMETER MISMATCH

(4), (5), and (7) are dependent on the motor parameters. But these parameters may not match with their actual values, affecting the performance of the MPCC method. The parameter mismatch can be reflected by adding uncertain components ΔR_s, ΔL_d, ΔL_q, and $\Delta\psi_m$ [41]. Referring to (4), the prediction model of the stator currents with parameter mismatch can be expressed as

$$\begin{cases} i_{dm}^p(k+1) = (1 - \dfrac{(R_s + \Delta R_s)T_s}{L_d + \Delta L_d}) i_d(k) \\ + \dfrac{\omega_e(k)(L_q + \Delta L_q)T_s i_q(k)}{L_d + \Delta L_d} + \dfrac{T_s u_d(k)}{L_d + \Delta L_d} \\ i_{qm}^p(k+1) = (1 - \dfrac{(R_s + \Delta R_s)T_s}{L_q + \Delta L_q}) i_q(k) \\ - \dfrac{\omega_e(k)(L_d + \Delta L_d)T_s i_d(k)}{L_q + \Delta L_q} + \dfrac{T_s u_q(k)}{L_q + \Delta L_q} \\ - \dfrac{\omega_e(k)(\psi_m + \Delta\psi_m)T_s}{L_q + \Delta L_q} \end{cases} \quad (8)$$

Considering that the predicted values of the dq-axis stator currents with the delay compensation are approximately equal to the reference values in the normal state and the measured values are approximately equal to the predicted values, the cost function with parameter mismatch can be developed as (9).

$$\begin{aligned} g_{im} = & [-\frac{R_s\Delta L_d - L_d\Delta R_s}{L_d(L_d + \Delta L_d)} T_s i_{dm}^p(k+1) \\ & + \frac{L_q\Delta L_d - L_d\Delta L_q}{L_d(L_d + \Delta L_d)} T_s i_{qm}^p(k+1)\omega_e(k+1) \\ & + \frac{\Delta L_d}{L_d(L_d + \Delta L_d)} T_s u_d(k+1)]^2 \\ & + [-\frac{R_s\Delta L_q - L_q\Delta R_s}{L_q(L_q + \Delta L_q)} T_s i_{qm}^p(k+1) \end{aligned}$$

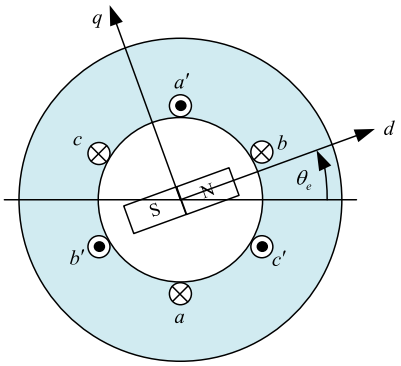

FIGURE 4. Motor construction with a single pole-pair on rotor.

$$
\begin{aligned}
&- \frac{L_d \Delta L_q - L_q \Delta L_d}{L_q(L_q + \Delta L_q)} T_s i^p_{dm}(k+1)\omega_e(k+1) \\
&+ \frac{\Delta L_q}{L_q(L_q + \Delta L_q)} T_s u_q(k+1) \\
&- \frac{\psi_m \Delta L_q - L_q \Delta \psi_m}{L_q(L_q + \Delta L_q)} T_s \omega_e(k+1)]^2 \\
&+ g[i^p_d(k+2), i^p_q(k+2)] \qquad (9)
\end{aligned}
$$

It can be seen that the parameter mismatch affects the cost function. In this case, the unexpected voltage vector is applied in the system, which will deteriorate the MPCC performance.

III. FAULT SIGNAL ANALYSIS

As seen in (9), the cost function is a fusion signal of the predicted value and the reference value of the dq-axis stator current, which can be used for the fault diagnosis. When the open-circuit fault occurs, the three-phase stator currents vary significantly. In this circumstance, the PMSM drive system may shift to one of the two possible operating states depending on the load torque. The motor stalls if the load torque is larger than the load capability of the faulted system. The other scenario is that the motor keeps operating with fluctuated torque and speed. This paper focuses on the latter one. In this section, the effect of an open power switch fault on the cost function is analyzed, using the T1's open-circuit fault as an example.

To facilitate the analysis of the current response in the fault state, the motor construction with a single pole-pair on the rotor is selected, as shown in Fig. 4. For the coordinates defined as in Fig. 4, the A-phase and permanent magnet fluxes are aligned when the rotor electrical angle θ_e is zero.

The voltage equations of the three-phase PMSM in abc-axis coordinate system are expressed as

$$
\begin{aligned}
v_A - v_N &= R_s i_a + L_s \frac{di_a}{dt} + M \frac{di_b}{dt} \\
&\quad + M \frac{di_c}{dt} - \sin\theta_e \omega_e \psi_m \qquad (10) \\
v_B - v_N &= R_s i_b + M \frac{di_a}{dt} + L_s \frac{di_b}{dt} \\
&\quad + M \frac{di_c}{dt} - \sin(\theta_e - \frac{2\pi}{3}) \omega_e \psi_m \qquad (11)
\end{aligned}
$$

$$
\begin{aligned}
v_C - v_N &= R_s i_c + M \frac{di_a}{dt} + M \frac{di_b}{dt} + L_s \frac{di_c}{dt} \\
&\quad - \sin(\theta_e + \frac{2\pi}{3}) \omega_e \psi_m \qquad (12)
\end{aligned}
$$

where v_A, v_B, and v_C are the phase voltages, v_N is the voltage of the neutral point of the three-phase stator winding, i_a, i_b, and i_c are the phase currents, L_s is the phase stator self-inductance, M is the mutual inductance between the stator phases, θ_e is rotor electrical angle.

A. ANALYSIS OF STATOR CURRENT AND DRIVE SIGNAL

The reference values of the dq-axis stator currents can be transformed to the abc-axis stator currents based on inverse Park's transformation, as expressed in (13).

$$
\begin{bmatrix} i^*_a \\ i^*_b \\ i^*_c \end{bmatrix} = \begin{bmatrix} \sin\theta_e & \cos\theta_e & 1 \\ \sin(\theta_e - 2\pi/3) & \cos(\theta_e - 2\pi/3) & 1 \\ \sin(\theta_e + 2\pi/3) & \cos(\theta_e + 2\pi/3) & 1 \end{bmatrix} \begin{bmatrix} i^*_p \\ i^*_d \\ 0 \end{bmatrix} \qquad (13)
$$

where i^*_d and i^*_q are the reference values of the dq-axis stator currents, i^*_a, i^*_b, and i^*_c are the reference values of the abc-axis stator currents.

The three-phase stator currents in normal can be expressed as

$$
\begin{cases}
i_a = I_m \sin(\theta) \\
i_b = I_m \sin(\theta - \frac{2}{3}\pi) \\
i_c = I_m \sin(\theta + \frac{2}{3}\pi)
\end{cases} \qquad (14)
$$

where I_m is the amplitude of the stator current, θ is the phase angle of the A-phase stator current. θ_e and θ satisfy the following relationship.

$$
\theta_e + \pi = \theta \qquad (15)
$$

When the open-circuit fault of T1 occurs, the three-phase stator currents vary greatly. The stator currents in fault state can be expressed as

$$
\begin{cases}
i'_a = I_m \sin(\theta) + x(\theta) \\
i'_b = I_m \sin(\theta - \frac{2}{3}\pi) + y(\theta) \\
i'_c = I_m \sin(\theta + \frac{2}{3}\pi) + z(\theta)
\end{cases} \qquad (16)
$$

where $x(\theta)$, $y(\theta)$, and $z(\theta)$ are the current variations after the fault happens.

Even if the drive signal of T1 is set high, the correct response current cannot be generated in the A-phase circuit due to the open-circuit fault of T1. There is a deviation between the reference value and the real value of the A-phase stator current. With the application of the MPCC method, the drive signal of T1 with $\theta_e \in (\pi, 2\pi]$ is always high, and T2 is off. The B-phase and C-phase circuits are normal, and their current response is timely. i'_b and i'_c are not always equal to zero. When θ_e is in the range $(\pi, 2\pi]$, the voltage vectors used to adjust the currents include $u_1(100)$, $u_2(110)$, and $u_6(101)$.

When $u_1(100)$ with $\theta_e \in (\pi, 2\pi]$ acts on three-phase stator circuits, no current flows through T1 due to an open-circuit

fault in T1. According to the sum of (10), (11), and (12), the following results can be obtained

$$0 - 3v_N = 0 \tag{17}$$

The neutral point voltage v_N is equal to zero according to (17). In addition, the back electromotive force of A-phase stator winding can be expressed as

$$e_a = -\sin\theta_e\omega_e\psi_m \geq 0 \quad \theta_e \in (\pi, 2\pi] \tag{18}$$

Based on (17) and (18), the voltage applied to both ends of the reverse diode in T2 is as follows

$$v'_A = v_N - \sin\theta_e\omega_e\psi_m \geq 0 \quad \theta_e \in (\pi, 2\pi] \tag{19}$$

From (19), it can be seen that the reverse diode in T2 does not conduct. Therefore, when $u_1(100)$ with $\theta_e \in (\pi, 2\pi]$ acts on three-phase stator circuits, i'_a is equal to zero. Similarly, the voltage vector $u_2(110)$ and $u_6(101)$ can be analyzed. When the open-circuit fault of T1 exists, i'_a with $\theta \in (0, \pi]$ can be considered equal to zero.

B. ANALYSIS OF COST FUNCTION

Based on Kirchhoff's current law, the sum of the three-phase stator currents flowing into the neutral point of the stator windings is 0. Before and after the occurrence of the fault, the sum of the stator currents can be expressed as

$$\begin{cases} i_a + i_b + i_c = 0 \\ i'_a + i'_b + i'_c = 0 \end{cases} \tag{20}$$

Since i'_a with $\theta \in (0, \pi]$ is equal to zero, the following relationship holds.

$$\begin{cases} i_a + x(\theta) = 0 \\ i_b + y(\theta) = -(i_c + z(\theta)) \quad \theta \in (0, \pi] \\ x(\theta) + y(\theta) + z(\theta) = 0 \end{cases} \tag{21}$$

The dq-axis stator currents in fault state are expressed as

$$\begin{cases} i'_d = i_d + \frac{2}{3}[\cos\theta_e x(\theta) + \cos(\theta_e - \frac{2}{3}\pi)y(\theta) \\ + \cos(\theta_e + \frac{2}{3}\pi)z(\theta)] \\ i'_q = i_q - \frac{2}{3}[\sin\theta_e x(\theta) + \sin(\theta_e - \frac{2}{3}\pi)y(\theta) \\ + \sin(\theta_e + \frac{2}{3}\pi)z(\theta)] \end{cases} \tag{22}$$

where i'_d and i'_q are the dq-axis stator currents.

The cost function in fault state is expressed as

$$g'_i = [i^*_d(k+2) - iq'^p(k+2)]^2 + [i^*_q(k+2) - i'_{qp}(k+2)]^2 + g[iq'^p(k+2), iq'^p(k+2)] \tag{23}$$

where $iq'^p(k+2)$ and $iq'^p(k+2)$ are the predicted values of the dq-axis stator currents in the fault state. Theoretically, the predicted values of the dq-axis stator currents are approximately equal to the reference values in the normal state, namely $i^*_d(k+2) \approx i^p_d(k+2)$ and $i^*_q(k+2) \approx i^p_q(k+2)$. The measured values are approximately equal to the predicted values, namely $i^p_d(k+2) \approx i_d(k+2)$ and $i^p_q(k+2) \approx i_q(k+2)$. The cost function in faulted state can be expressed as

$$\begin{aligned} g'_i = \frac{4}{9}[&\cos(\theta_e(k+2))\, x(\theta(k+2)) \\ &+ \cos\left(\theta_e(k+2) - \frac{2}{3}\pi\right) y(\theta(k+2)) \\ &+ \cos\left(\theta_e(k+2) + \frac{2}{3}\pi\right) z(\theta(k+2))\Big]^2 \\ &+ \frac{4}{9}[\sin(\theta_e(k+2))\, x(\theta(k+2)) \\ &+ \sin\left(\theta_e(k+2) - \frac{2}{3}\pi\right) y(\theta(k+2)) \\ &+ \sin\left(\theta_e(k+2) + \frac{2}{3}\pi\right) z(\theta(k+2))\Big]^2 \\ &+ g\left[i'^p_d(k+2), i'^p_q(k+2)\right] \end{aligned} \tag{24}$$

Assuming that g'_i is equal to zero, $x(\theta)$, $y(\theta)$, and $z(\theta)$ with $\theta_e \in (0, 2\pi]$ are equal. The analysis result of this hypothesis is contradictory to the analysis result of the T1's open-circuit fault. Therefore, the hypothesis does not hold. Under T1's open-circuit fault condition, g'_i with $\theta \in (0, \pi]$ is greater than 0. The cost function can be used for anomaly detection of the PMSM drive system.

IV. FAULT DETECTION AND IDENTIFICATION

Ideally, based on the analysis in Section III, the cost function is near zero under healthy conditions. However, to avoid false detection, the preset threshold should be set reasonably. In this paper, the Boolean variable used for anomaly detection of the PMSM drive system is defined as follows

$$\varepsilon = \begin{cases} 1 & g_i > g_{th} \\ 0 & otherwise \end{cases} \tag{25}$$

where ε is the generated Boolean variable, g_{th} is the preset threshold.

Once the system's anomaly is detected, the faulty power switch is required to be identified. The magnitudes of the three-phase stator currents are defined, specifically $d_a = |i_a|$, $d_b = |i_b|$, and $d_c = |i_c|$. Assuming that the T1's open-circuit fault occurs, d_a, d_b, and d_c vary significantly. In the range $(0,\pi]$ of the phase angle of the A-phase stator current, $d_a \approx 0$. Hence, the phase circuit where the faulty power switch is can be identified. Considering the response current deviation of the PMSM drive system with the MPCC method, the Boolean variable used for phase circuit identification is defined as

$$\varepsilon_i = \begin{cases} 1 & d_i < d_{th} \\ 0 & otherwise \end{cases} \tag{26}$$

where $i = a, b, c$, d_{th} is the set threshold. When a certain power switch fails, its driving signal is abnormal in the MPCC method. For example, for an open-circuit fault of T1, the T1's driving signal is high level in $\theta \in (0, \pi]$. The Boolean

TABLE 1. *Flag*, $Flag_i$, and $Flag_j$ under healthy and fault conditions.

State	$Flag$	$Flag_i$			$Flag_j$					
		$Flag_a$	$Flag_b$	$Flag_c$	$Flag_{s1}$	$Flag_{s2}$	$Flag_{s3}$	$Flag_{s4}$	$Flag_{s5}$	$Flag_{s6}$
Healthy	0	0	0	0	-	-	-	-	-	-
T1 open fault	1	1	0	0	1	0	-	-	-	-
T2 open fault	1	1	0	0	0	1	-	-	-	-
T3 open fault	1	0	1	0	-	-	1	0	-	-
T4 open fault	1	0	1	0	-	-	0	1	-	-
T5 open fault	1	0	0	1	-	-	-	-	1	0
T6 open fault	1	0	0	1	-	-	-	-	0	1

variable used to identify the faulty power switch is defined as

$$\varepsilon_j = \begin{cases} 1 & \mathrm{S}_j = 1 \\ 0 & otherwise \end{cases} \tag{27}$$

where $j = 1, 2, 3, 4, 5, 6$, and S_j is the drive signal.

Moreover, considering that the operating conditions of the PMSM drive system are constantly changing, and the current signal may be affected by the noise, the fault detection and identification based on (25), (26), and (27) may be false. Hence, the counting filter algorithm is applied to improve the practicability, in which a counter triggered by suspected current overrun starts incrementing till a preset count value. Based on the dynamic performance analysis of the motor drive system, the preset count *Count* is set reasonably, and $Count < (T_{\omega e}/(2T_s))$, where $T_{\omega e}$ is stator current period, and T_s is the sampling period. A larger value of *Count* leads to a longer time for fault detection, while a smaller one affects the reliability. In this case, the flags for fault detection and identification of power switches are expressed as

$$Flag = \begin{cases} 1 & \frac{counter1}{Count} > K_1 \\ 0 & otherwise \end{cases} \tag{28}$$

$$Flag_i = \begin{cases} 1 & \frac{counter2}{Count} > K_2 \\ 0 & otherwise \end{cases} \tag{29}$$

$$Flag_j = \begin{cases} 1 & \frac{counter3}{Count} > K_3 \\ 0 & otherwise \end{cases} \tag{30}$$

where *Flag*, $Flag_i$, and $Flag_j$ are the fault detection and identification flags. *counter*1 is the counter value from the beginning of the detection of the Boolean variable $\varepsilon = 1$ in (25) to the arriving at the constant *Count*. If $(counter1/Count)$ is larger than the set threshold K_1, the *Flag* is set from low to high. In addition, $(counter2, K_2, Flag_i)$ and$(counter3, K_3, Flag_j)$ have similar definitions to $(counter1, K_1, Flag)$. Therefore, the open circuit fault of the power switches can be diagnosed by *Flag*, $Flag_i$, and $Flag_j$, as shown in Table 1. Moreover, a block diagram illustrating the diagnosis method for semiconductor power switch open circuit fault is shown in Fig. 5.

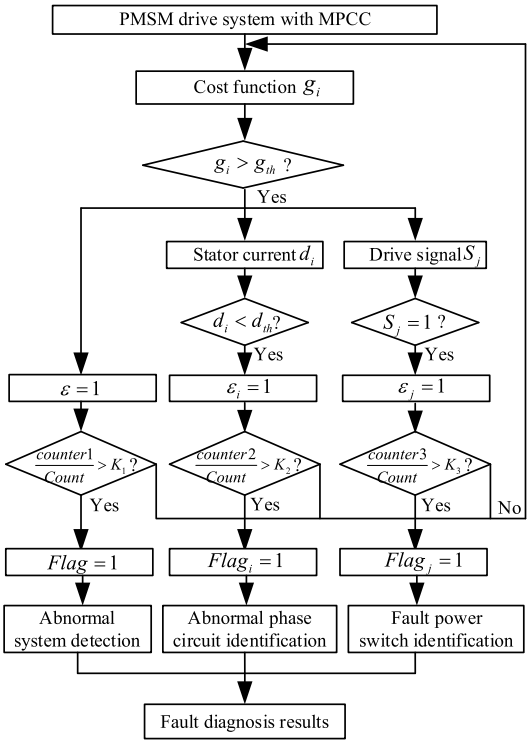

FIGURE 5. Fault diagnosis block diagram for PMSM drive system with MPCC.

TABLE 2. Parameters of the studied PMSM drive system model.

Parameters	Symbol	Value
Number of pole pairs	p	4
Magnet flux linkage	ψ_m	0.48333Wb
q-axis inductance	L_q	0.002H
d-axis inductance	L_d	0.002H
Phase resistance	R_s	0.31Ω
DC voltage source	v_{dc}	270V
Signal sampling frequency	f_s	40kHz
IGBT switching frequency	f_{sw}	40kHz

V. SIMULATION RESULTS

The MATLAB/Simulink model of the studied PMSM drive system with the MPCC method is shown in Fig. 6. The system's parameters are listed in Table 2. In the built model, the power switch is turned off to emulate its open-circuit fault. Besides, it has been validated that the three-phase stator

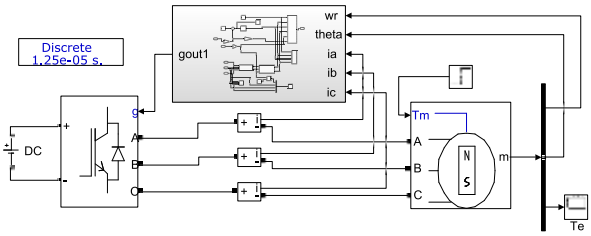

FIGURE 6. Simulation model of the studied PMSM drive system with the MPCC method.

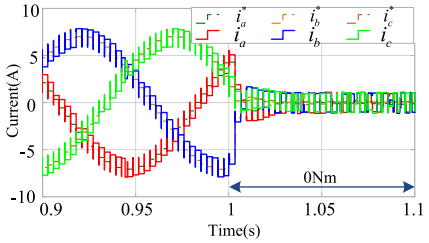

FIGURE 7. Three-phase stator currents and the MPCC references.

currents can track the MPCC reference with an ignorable deviation Δi under the healthy condition, as shown in Fig. 7.

For diagnosis in fault conditions, the threshold g_{th} and d_{th} is determined based on the cost function $g_{0\max}$ and the deviation $\Delta i_{0\max}$ under 0 Nm operation condition. Based on (4), assuming that the initial values of both currents and speed are 0, the deviation $\Delta i_{0d\max}$ and $\Delta i_{0q\max}$ can be derived as follows.

$$\Delta i_{0d\max} = \frac{T_s u_d}{L_d}, \Delta i_{0q\max} = \frac{T_s u_q}{L_q}.$$

So, $\Delta i_{0\max} = \sqrt{\Delta i_{0d\max}^2 + \Delta i_{0q\max}^2}$, $g_{0\max} = \Delta i_{0d\max}^2 + \Delta i_{0q\max}^2$.

In the studied cases, $g_{th} = 5$, $d_{th} = 2.25$, $Count = T_{\omega e}/(3T_s)$, $K_1 = 0.9$, $K_2 = 0.9$, $K_3 = 0.9$.

A. CONSTANT TORQUE AND CONSTANT SPEED OPERATING CONDITION

Fig. 8 shows simulation results of the PMSM drive system with T1 open-circuit fault at 30Nm/700rpm. At the instant $t = 1s$, T1's open-circuit fault is introduced. Under the healthy condition, the stator currents are symmetrical, the cost function is stable and small, and the drive signals of T1 and T2 are constantly changing. In addition, the fault detection and identification flags are equal to zero under the healthy condition. When T1's open-circuit fault exists, the stator currents change obviously. Within half an electrical angle period, the A-phase stator current is distributed near zero. The cost function is obviously larger than the maximum value under normal conditions. T1's drive signal keeps high. In the other half electrical angle period, the response currents gradually return to normal. Moreover, at the instant $t = 1.008675s$, the flags $Flag$, $Flag_a$, and $Flag_1$ are both changed

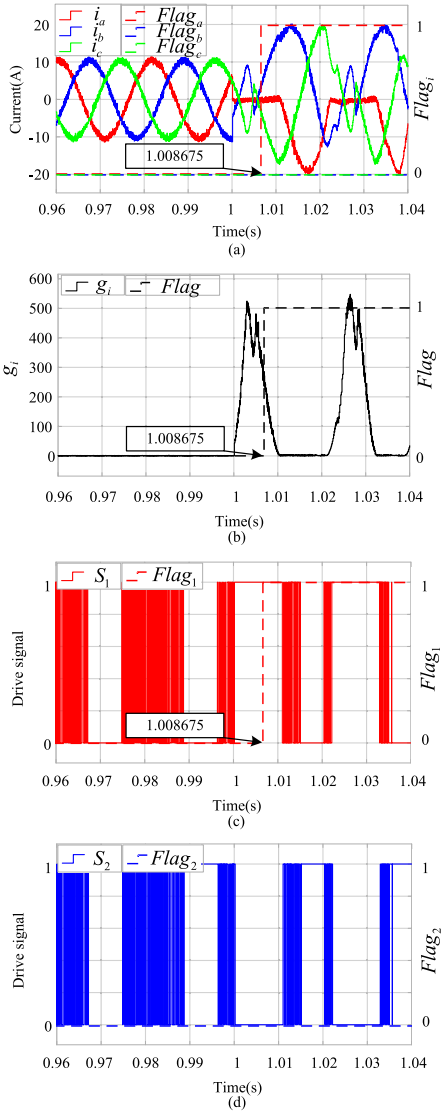

FIGURE 8. Simulation results of PMSM drive system with T1 open circuit fault at 30Nm/700rpm (a) Stator currents and $Flag_i$ (b) Cost function and $Flag$ (c) Drive signal and $Flag_1$ (d) Drive signal and $Flag_2$.

to 1. Therefore, the simulation results show that based on the flags $Flag$, $Flag_i$, and $Flag_j$, the open circuit fault of the power switch can be diagnosed. The effectiveness of the fault diagnosis method is verified at constant torque and constant speed operating conditions.

B. VARIABLE TORQUE AND VARIABLE SPEED OPERATING CONDITION

To verify the robustness of the proposed fault diagnosis method, the simulation results of fault detection of the PMSM drive system under variable torque and variable speed operation conditions should be analyzed. In this part, the torque changes from 15Nm to 30Nm, and the speed changes from 350rpm to 700rpm within 0.9s-1.1s. The simulation results are shown as Fig. 9. At the instant $t = 1s$, T1's open-circuit fault is introduced. In this current electrical angle period,

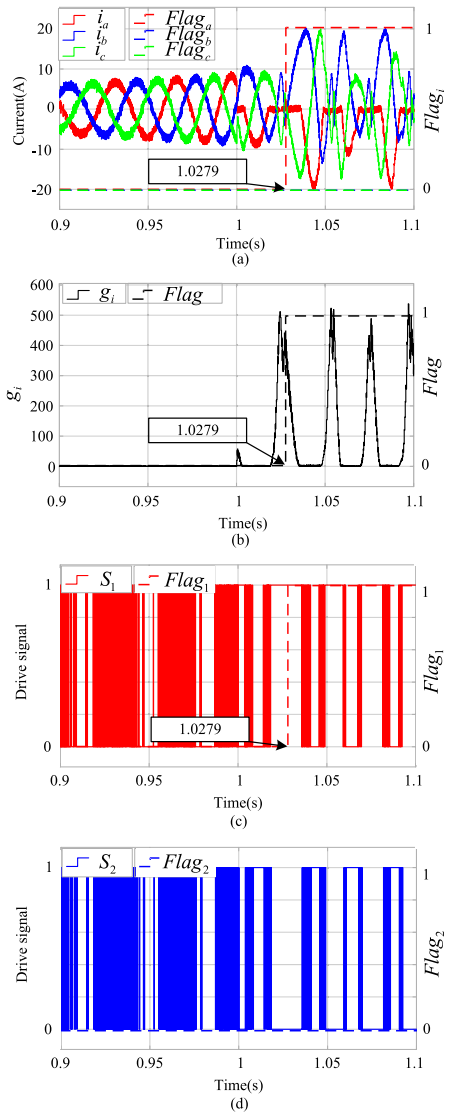

FIGURE 9. Simulation results of PMSM drive system with T1 open circuit fault at (15-30)Nm/(350-700)rpm (a) Stator currents and $Flag_i$ (b) Cost function and *Flag* (c) Drive signal and $Flag_1$ (d) Drive signal and $Flag_2$.

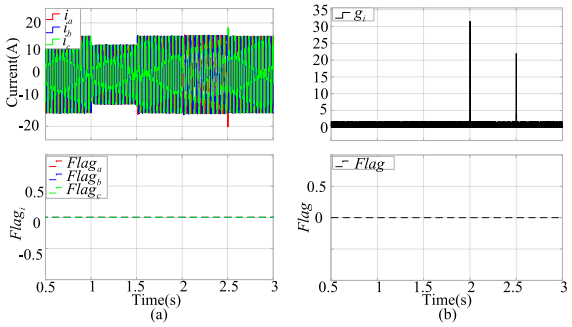

FIGURE 10. Simulation results of PMSM drive system during transient condition(a) Stator currents and $Flag_i$ (b) Cost function and *Flag*.

the fault information is not enough to complete the fault diagnosis process, but in the next electrical angle period, the flags *Flag*, $Flag_a$, and $Flag_1$ are both equal to 1 at the instant

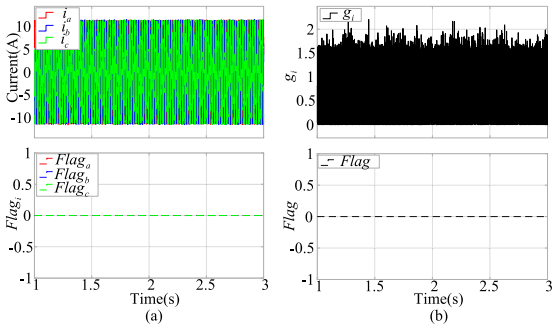

FIGURE 11. Simulation results of PMSM drive system under phase resistance variation (a) Stator currents and $Flag_i$ (b) Cost function and *Flag*.

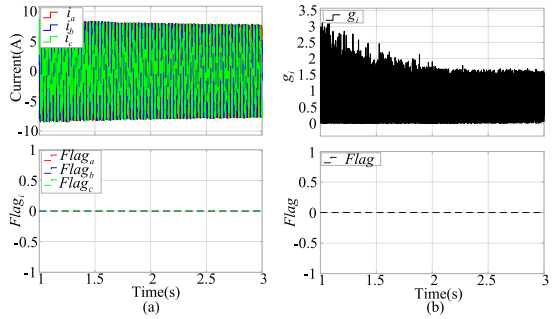

FIGURE 12. Simulation results of PMSM drive system under inductance variation (a) Stator currents and $Flag_i$ (b) Cost function and *Flag*.

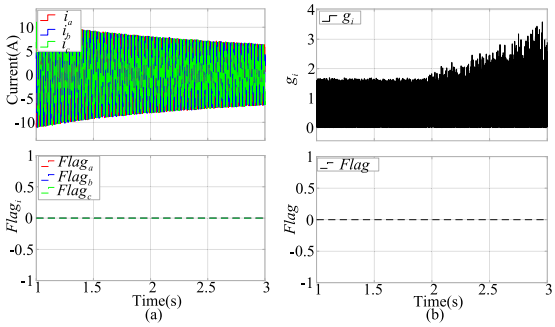

FIGURE 13. Simulation results of PMSM drive system under permanent magnet flux linkage variation (a) Stator currents and $Flag_i$ (b) Cost function and *Flag*.

$t = 1.0279s$. The T1's open-circuit fault can be diagnosed in time. Therefore, the robustness of the fault diagnosis method is verified under the variable torque and variable speed operating condition.

C. TRANSIENT BEHAVIOR

Fig. 10 shows the simulation results of the PMSM drive system during the transient condition, which is used to verify the performance of the proposed fault diagnosis method. At the instant $t = 1s$, the load torque changed from 40 Nm to 30 Nm, and then changed back to 40Nm. In addition, at the instant $t = 2s$, the reference speed changed from 400rpm to 300rpm. At the instant $t = 2.5s$, the reference speed

changed back to 400rpm. As the reference speed and the load torque changed, three-phase stator currents and the cost function have transient processes. This situation is affected by the PMSM drive system control strategy. The flags *Flag* and $Flag_i$ are still equal to zero. Hence, Fig. 10 shows that the proposed fault diagnosis method is insensitive to the speed and load transient.

D. EFFECT OF PARAMETER MISMATCH

Based on (4), the cost function includes the predicted values of the stator currents, which is dependent on the parameters of the PMSM, mainly including the phase resistance, dq-axis inductances, and permanent magnet flux linkage. These parameters are subject to small changes due to temperature and other factors. Therefore, it is necessary to investigate the influence of PMSM parameter mismatch on the fault diagnosis method.

Figs. 11-13 show the simulation results of the PMSM drive system at 20Nm/500rpm with the different values of phase resistance, dq-axis inductances, and permanent magnet flux linkage. In this paper, the range of parameter variation is from −30% to 30% of the normal parameter value. And the flags *Flag* and $Flag_i$ maintains zero. The PMSM parameter mismatch can deteriorate the MPCC performance, however, it has little effect on the proposed fault diagnosis method.

VI. CONCLUSION

This paper proposes an open-circuit fault diagnosis method of semiconductor power switch for the PMSM drive system with the MPCC method. A thorough analysis has been carried out based on the analytical model of the PMSM to select the calculated result of the cost function of the MPCC algorithm as the primary fault characteristic parameter. It is found that a suspected fault state of the PMSM drive system can be firstly judged by whether the calculated value of the cost function exceeds a preset threshold. The system's abnormality can be further confirmed by the identification flags, which is the results of a digital counting filter algorithm according to the monitoring stator current and the gate-driving signals of the power switches. The simulation results have verified the effectiveness and robustness of the proposed fault diagnosis method of the open-circuit fault of the power switches in the PMSM driving system.

REFERENCES

[1] X. Zhu, Z. Xiang, L. Quan, W. Wu, and Y. Du, "Multimode optimization design methodology for a flux-controllable stator permanent magnet memory motor considering driving cycles," *IEEE Trans. Ind. Electron.*, vol. 65, no. 7, pp. 5353–5366, Jul. 2018, doi: 10.1109/TIE.2017.2777408.

[2] J. Hang, M. Xia, S. Ding, Y. Li, L. Sun, and Q. Wang, "Research on vector control strategy of surface-mounted permanent magnet synchronous machine drive system with high-resistance connection," *IEEE Trans. Power Electron.*, vol. 35, no. 2, pp. 2023–2033, Feb. 2020, doi: 10.1109/TPEL.2019.2918683.

[3] W. Wang, M. Cheng, B. Zhang, Y. Zhu, and S. Ding, "A fault-tolerant permanent-magnet traction module for subway applications," *IEEE Trans. Power Electron.*, vol. 29, no. 4, pp. 1646–1658, Apr. 2014, doi: 10.1109/TPEL.2013.2266377.

[4] F. Guo and F. Zhang, "A study of driving cycle for electric cars on Beijing urban and suburban roads," in *Proc. IEEE Int. Conf. Power Renew. Energy (ICPRE)*, Shanghai, China, Oct. 2016, pp. 319–322, doi: 10.1109/ICPRE.2016.7871224.

[5] C.-Y. Lin, P.-L. Li, C.-H. Li, and W.-S. Chiang, "Investigation on IGBT failure effects of EV/HEV inverter using fault insertion HiL testing," in *Proc. Int. Electr. Vehicle Symp. Exhib.*, KINTEX, Gyeonggi-do, South Korea, 2015, pp. 1–9.

[6] J. Hang, H. Wu, S. Ding, W. Hua, and Q. Wang, "A DC-flux-injection method for fault diagnosis of high-resistance connection in direct-torque-controlled PMSM drive system," *IEEE Trans. Power Electron.*, vol. 35, no. 3, pp. 3029–3042, Mar. 2020, doi: 10.1109/TPEL.2019.2924929.

[7] S. Yang, A. Bryant, P. Mawby, D. Xiang, L. Ran, and P. Tavner, "An industry-based survey of reliability in power electronic converters," *IEEE Trans. Ind. Appl.*, vol. 47, no. 3, pp. 1441–1451, May/Jun. 2011, doi: 10.1109/TIA.2011.2124436.

[8] B. Lu and S. Sharma, "A survey of IGBT fault diagnostic methods for three-phase power inverters," in *Proc. Int. Conf. Condition Monit. Diagnosis*, Beijing, China, 2008, pp. 756–763, doi: 10.1109/CMD.2008.4580396.

[9] B. Lu and S. Sharma, "A literature review of IGBT fault diagnostic and protection methods for power inverters," *IEEE Trans. Ind. Appl.*, vol. 45, no. 5, pp. 1770–1777, Sep./Oct. 2009, doi: 10.1109/TIA.2009.2027535.

[10] D. U. Campos-Delgado and D. R. Espinoza-Trejo, "An observer-based diagnosis scheme for single and simultaneous open-switch faults in induction motor drives," *IEEE Trans. Ind. Electron.*, vol. 58, no. 2, pp. 671–679, Feb. 2011, doi: 10.1109/TIE.2010.2047829.

[11] S.-M. Jung, J.-S. Park, H.-W. Kim, K.-Y. Cho, and M.-J. Youn, "An MRAS-based diagnosis of open-circuit fault in PWM voltage-source inverters for PM synchronous motor drive systems," *IEEE Trans. Power Electron.*, vol. 28, no. 5, pp. 2514–2526, May 2013, doi: 10.1109/TPEL.2012.2212916.

[12] X. Zhou, J. Sun, P. Cui, Y. Lu, M. Lu, and Y. Yu, "A fast and robust open-switch fault diagnosis method for variable-speed PMSM system," *IEEE Trans. Power Electron.*, vol. 36, no. 3, pp. 2598–2610, Mar. 2021, doi: 10.1109/TPEL.2020.3013628.

[13] T. Chen, Y. Pan, and Z. Xiong, "A hybrid system model-based open-circuit fault diagnosis method of three-phase voltage-source inverters for PMSM drive systems," *Electronics*, vol. 9, no. 8, p. 1251, Aug. 2020, doi: 10.3390/electronics9081251.

[14] F. Naseri, E. Schaltz, K. Lu, and E. Farjah, "Real-time open-switch fault diagnosis in automotive permanent magnet synchronous motor drives based on Kalman filter," *IET Power Electron.*, vol. 13, no. 12, pp. 2413–2423, Sep. 2020, doi: 10.1049/iet-pel.2019.1498.

[15] R. Wang, Q. Sun, D. Ma, and Z. Liu, "The small-signal stability analysis of the droop-controlled converter in electromagnetic timescale," *IEEE Trans. Sustain. Energy*, vol. 10, no. 3, pp. 1459–1469, Jul. 2019, doi: 10.1109/TSTE.2019.2894633.

[16] K. Rothenhagen and F. W. Fuchs, "Performance of diagnosis methods for IGBT open circuit faults in voltage source active rectifiers," in *IEEE Annu. Power Electron. Spec. Conf.*, vol. 6, Aachen, Germany, Jun. 2004, pp. 4348–4354, doi: 10.1109/PESC.2004.1354769.

[17] S. Abramik, W. Sleszynski, J. Nieznanski, and H. Piquet, "A diagnostic method for on-line fault detection and localization in VSI-fed AC drives," in *Proc. Eur. Conf. Power Electron. Appl. (EPE)*, 2003, pp. 1–9.

[18] A. M. S. Mendes and A. J. M. Cardoso, "Voltage source inverter fault diagnosis in variable speed AC drives, by the average current Park's vector approach," in *Proc. IEEE Int. Electr. Mach. Drives Conf.*, Seattle, WA, USA, May 1999, pp. 704–706, doi: 10.1109/IEMDC.1999.769220.

[19] J. O. Estima and A. J. M. Cardoso, "A new approach for real-time multiple open-circuit fault diagnosis in voltage source inverters," in *Proc. IEEE Energy Convers. Congr. Expo.*, Atlanta, GA, USA, Sep. 2010, pp. 4328–4335, doi: 10.1109/ECCE.2010.5618462.

[20] J. O. Estima and A. J. M. Cardoso, "A new approach for real-time multiple open-circuit fault diagnosis in voltage-source inverters," *IEEE Trans. Ind. Appl.*, vol. 47, no. 6, pp. 2487–2494, Nov./Dec. 2011, doi: 10.1109/TIA.2011.2168800.

[21] L. Yu, Y. Zhang, W. Huang, and K. Teffah, "A fast-acting diagnostic algorithm of insulated gate bipolar transistor open circuit faults for power inverters in electric vehicles," *Energies*, vol. 10, no. 4, p. 552, Apr. 2017, doi: 10.3390/en10040552.

[22] H. Wei, Y. Zhang, L. Yu, M. Zhang, and K. Teffah, "A new diagnostic algorithm for multiple IGBTs open circuit faults by the phase currents for power inverter in electric vehicles," *Energies*, vol. 11, no. 6, p. 1508, Jun. 2018, doi: 10.3390/en11061508.

[23] S. K. E. Khil, I. Jlassi, A. J. M. Cardoso, J. O. Estima, and N. Mrabet-Bellaaj, "Diagnosis of open-switch and current sensor faults in PMSM drives through stator current analysis," *IEEE Trans. Ind. Appl.*, vol. 55, no. 6, pp. 5925–5937, Nov. 2019, doi: 10.1109/TIA.2019.2930592.
[24] W. Sleszynski, J. Nieznanski, and A. Cichowski, "Open-transistor fault diagnostics in voltage-source inverters by analyzing the load currents," *IEEE Trans. Ind. Electron.*, vol. 56, no. 11, pp. 4681–4688, Nov. 2009, doi: 10.1109/TIE.2009.2023640.
[25] H. Yan, Y. Xu, F. Cai, H. Zhang, W. Zhao, and C. Gerada, "PWM-VSI fault diagnosis for a PMSM drive based on the fuzzy logic approach," *IEEE Trans. Power Electron.*, vol. 34, no. 1, pp. 759–768, Jan. 2019, doi: 10.1109/TPEL.2018.2814615.
[26] X. Hu, H. Zhang, D. Ma, and R. Wang, "A tnGAN-based leak detection method for pipeline network considering incomplete sensor data," *IEEE Trans. Instrum. Meas.*, vol. 70, pp. 1–10, 2021, doi: 10.1109/TIM.2020.3045843.
[27] T. Shi, Y. He, T. Wang, and B. Li, "Open switch fault diagnosis method for PWM voltage source rectifier based on deep learning approach," *IEEE Access*, vol. 7, pp. 66595–66608, 2019, doi: 10.1109/ACCESS.2019.2917311.
[28] Z. Y. Xue, K. S. Xiahou, M. S. Li, T. Y. Ji, and Q. H. Wu, "Diagnosis of multiple open-circuit switch faults based on long short-term memory network for DFIG-based wind turbine systems," *IEEE J. Emerg. Sel. Topics Power Electron.*, vol. 8, no. 3, pp. 2600–2610, Sep. 2020, doi: 10.1109/JESTPE.2019.2908981.
[29] S. S. Moosavi, A. Kazemi, and H. Akbari, "A comparison of various open-circuit fault detection methods in the IGBT-based DC/AC inverter used in electric vehicle," *Eng. Failure Anal.*, vol. 96, pp. 223–235, Feb. 2019, doi: 10.1016/j.engfailanal.2018.09.020.
[30] B. Cai, Y. Zhao, H. Liu, and M. Xie, "A data-driven fault diagnosis methodology in three-phase inverters for PMSM drive systems," *IEEE Trans. Power Electron.*, vol. 32, no. 7, pp. 5590–5600, Jul. 2017, doi: 10.1109/TPEL.2016.2608842.
[31] Z. Li, Y. Gao, X. Zhang, B. Wang, and H. Ma, "A model-data-hybrid-driven diagnosis method for open-switch faults in power converters," *IEEE Trans. Power Electron.*, vol. 36, no. 5, pp. 4965–4970, May 2021, doi: 10.1109/TPEL.2020.3026176.
[32] M. Siami, D. A. Khaburi, and J. Rodriguez, "Simplified finite control set-model predictive control for matrix converter-fed PMSM drives," *IEEE Trans. Power. Electron.*, vol. 33, no. 3, pp. 2438–2446, Mar. 2018, doi: 10.1109/TPEL.2017.2696902.
[33] S. Chai, L. Wang, and E. Rogers, "A cascade MPC control structure for a PMSM with speed ripple minimization," *IEEE Trans. Ind. Electron.*, vol. 60, no. 8, pp. 2978–2987, Aug. 2013, doi: 10.1109/TIE.2012.2201432.
[34] C. Gong, Y. Hu, K. Ni, J. Liu, and J. Gao, "SM load torque observer-based FCS-MPDSC with single prediction horizon for high dynamics of surface-mounted PMSM," *IEEE Trans. Power Electron.*, vol. 35, no. 1, pp. 20–24, Jan. 2020, doi: 10.1109/TPEL.2019.2929714.
[35] T. Geyer, R. P. Aguilera, and D. E. Quevedo, "On the stability and robustness of model predictive direct current control," in *Proc. IEEE Int. Conf. Ind. Technol. (ICIT)*, Cape Town, South Africa, Feb. 2013, pp. 374–379, doi: 10.1109/ICIT.2013.6505701.
[36] Y. Zhang and H. Yang, "Two-vector-based model predictive torque control without weighting factors for induction motor drives," *IEEE Trans. Power Electron.*, vol. 31, no. 2, pp. 1381–1390, Feb. 2016, doi: 10.1109/TPEL.2015.2416207.
[37] J. Hang, H. Wu, J. Zhang, S. Ding, Y. Huang, and W. Hua, "Cost function-based open-phase fault diagnosis for PMSM drive system with model predictive current control," *IEEE Trans. Power Electron.*, vol. 36, no. 3, pp. 2574–2583, Mar. 2021, doi: 10.1109/TPEL.2020.3011450.
[38] J. Hang, J. Zhang, M. Xia, S. Ding, and W. Hua, "Interturn fault diagnosis for model-predictive-controlled-PMSM based on cost function and wavelet transform," *IEEE Trans. Power Electron.*, vol. 35, no. 6, pp. 6405–6418, Jun. 2020, doi: 10.1109/TPEL.2019.2953269.
[39] B. Gmati, I. Jlassi, S. K. E. Khil, and A. J. M. Cardoso, "Open-switch fault diagnosis in voltage source inverters of PMSM drives using predictive current errors and fuzzy logic approach," *IET Power Electron.*, vol. 14, no. 6, pp. 1059–1072, May 2021, doi: 10.1049/pel2.12098.
[40] W. Huang, J. Du, W. Hua, W. Lu, K. Bi, Y. Zhu, and Q. Fan, "Current-based open-circuit fault diagnosis for PMSM drives with model predictive control," *IEEE Trans. Power Electron.*, vol. 36, no. 9, pp. 10695–10704, Sep. 2021, doi: 10.1109/TPEL.2021.3061448.
[41] X. Yuan, S. Zhang, C. Zhang, A. Galassini, G. Buticchi, and M. Degano, "Improved model predictive current control for SPMSM drives using current update mechanism," *IEEE Trans. Ind. Electron.*, vol. 68, no. 3, pp. 1938–1948, Mar. 2021, doi: 10.1109/TIE.2020.2973880.

HAI YU received the B.S. degree in electrical engineering from Shandong University of Science and Technology, Qingdao, Shandong, China, in 2013, and the M.S. degree in electrical engineering from Lanzhou University of Technology, Lanzhou, Gansu, China, in 2016. He is currently pursuing the Ph.D. degree in mechanical engineering with Beijing Institute of Technology, Beijing, China. His research interests include performance analysis of permanent magnet synchronous motor drive system based on real-world big data and fault diagnosis of permanent magnet synchronous motor drive systems.

JUNJUN DENG (Member, IEEE) received the B.S., M.S., and Ph.D. degrees in electrical engineering from Northwestern Polytechnical University, Xi'an, China, in 2008, 2011, and 2015, respectively. From 2011 to 2014, he was a Visiting Scholar with the Department of Electrical and Computer Engineer, University of Michigan, Dearborn. In 2016, he has joined the Faculty of Vehicle Engineering, Beijing Institute of Technology, Beijing, China. His research interests include wireless power transfer, motor drive, and high performance battery chargers for electric vehicles.

YANG LI received the B.S. and M.S. degrees in software engineering from Beijing University of Posts and Telecommunications, Beijing, China. He is currently pursuing the Ph.D. degree in mechanical engineering with Beijing Institute of Technology, Beijing. He is currently an Executive Secretary with the Chinese National Big Data Alliance of New Energy Vehicles and participates in the Key Consulting Project with the Chinese Academy of Engineering. His research interests include NEV industry policy research, scientific project management, and big-data analysis for electric vehicles.